American Chemical Science Journal
4(5): 687-705, 2014

SCIENCEDOMAIN *international*
www.sciencedomain.org

Kinetics of Divalent Metals (Cd^{2+}, Cu^{2+}, Pb^{2+}, Zn^{2+}) Adsorption onto a Modified Brick

O. Allahdin[1], M. Wartel[2], J. Mabingui[1] and A. Boughriet[2,3*]

[1]*UNESCO Chair"On Water Management," Lavoisier Hydrosciences Laboratory, University of Bangui, Faculty of Science, PO Box 908, Central African Republic.*
[2]*University of Lille 1, Geosystems Laboratory, Analytical Chemistry and Marine Team, UMR CNRS8217, BâtC8, 59655 Villeneuve d'Ascq Cedex, France.*
[3]*University Lille Nord de France, IUT Bethune Department of Chemistry, University Street, BP819, 62408BethuneCedex, France.*

Authors' contributions

This work was carried out in collaboration between all authors. This experimental work was performed by author OA as part of his thesis. Authors MW and AB supervised the work. Author AB collected experimental data and wrote the manuscript. Author JM was at the origin of this research project and helped to gain financial supports as government principal private secretary (State Minister) in Central African Republic. All authors read and approved the final manuscript.

Original Research Article

Received 31st January 2014
Accepted 23rd March 2014
Published 15th May 2014

ABSTRACT

Brick which originated from Bangui Region (in Central African Republic), was pre-activated with HCl at 90°C and coated with ferrihydrite. This material was used in the present work as an adsorbent mainly for the removal of metallic cations (Me^{2+} = Cd^{2+}; Cu^{2+}; Pb^{2+}; Zn^{2+}) from aqueous solutions due to their bad effect on the environment. Experimental results were compared to those obtained for other divalent cations (Ca^{2+}, Fe^{2+}, Mg^{2+}, Mn^{2+}, Sr^{2+}). Freundlich and Langmuir models were applied to describe adsorptions isotherms, and Langmuir model was found to provide the best fitting. Langmuir adsorption capacities (Q_{max}) of these ions onto ferrihydrite-coated brick increased in the following order: Cu > Zn >Pb>Ca> Cd >Mg. Kinetic studies revealed that experimental data were better fitted by the pseudo second-order rate equation than the pseudo first-order rate one. Thermodynamic analyses indicated that the adsorption kinetics process was endothermic. Because of acid/hydrolysis characteristics of metallic

**Corresponding author: Email: abdel.boughriet@univ-lille1.fr;*

cations, the kinetic constant, k_2, was found to be affected by H^+ and OH^- (*i.e.,* solution pH) as potential-determining ions by regulating proportions of negative and positive charges at the brick surface. The adsorption capacity (Qe) was determined from kinetic data and the adsorption affinity of the studied eight elements onto ≡S-OH sites in modified brick had the following order: Pb> Cu > Cd ≈ Mn ≈ Zn > Mg >Ca> Sr. These Qevalues were found to be instead related to the surface binding constant, $K_{(\equiv SOMe)}$, relative to the equilibrium: (≡S-OH) + Me^{2+} ↔ (≡S-O)Me^+ + H^+), suggesting the implication of hydroxyl groups from brick metakaolinite in addition to –OH and/or –ONa functions mainly present in ferrihydrite deposits.

Keywords: Brick; ferrihydrite; metakaolinite; divalent cation; adsorption; isotherm; kinetics; complexation.

1. INTRODUCTION

Aqueous metal ions are known to be toxic, even at very low concentrations, and their presence in wastewaters, ground waters for instance, the maximum acceptable concentration of Cd^{++}, Cu^{++}, Zn^{++} and Pb^{++} recommended by the World Health Organization (WHO) for drinking water is : 3µg/L, 10µg/L, 3µg/L and 2 µg/L, respectively . High levels of these metals pose risks to human health, mainly : *Cadmium*, because of its carcinogenic, mutagenic and teratogenic effects, and as endocrine disruptor and it causes chronic anemia and renal failure; *Copper*, it causes brain and kidney damages, chronic anemia, liver cirrhosis, and stomach/intestinal irritations; *Zinc*, it can cause dizziness and fatigue; and *Lead*, because of its harmful effects on the development, intelligence and memory of children, and it is also known to increase the risks of renal failure and cardiovascular disease [1]. This explains why the removal of metal ions from aqueous solutions is nowadays considered as one of the great problems on water treatments worldwide. To remove heavy metals from contaminated waters, numerous purification-treatment technologies have been developed over the last decades [2-8]. Among them, adsorption has gained importance for this task, and some natural materials (such as: chitosan, fly ash, coal, zeolite, clays, agricultural waste materials) have been used successfully as low-cost adsorbents [9-12]. To enhance the sorption of these natural adsorbents towards heavy metals, chemical modifications of their surfaces with metal oxide(s) /hydroxide(s) have often been made [13]. For instance, the impregnation of zeolite with iron (or manganese) oxides resulted in high removal efficiency of copper(II) and lead(II) from aqueous solutions [14-16].

On this view, we have recently proposed brick as a low cost, no toxicity, easily available, effective and reusable adsorbents for the removal of metal cations from aqueous environment [17-21]. Thus, water treatments based on using modified brick is now tested in rural areas of Central African Republic where this material (which is commonly made by local craftsmen) can be obtained by African population in large quantities and cheap. This brick is mainly composed of sand and metakaolinite, and to a lesser extent, of iron oxides [17]. Moreover, iron oxide / hydroxide used alone as a separate phase is commonly referred as an adsorbent to remove metal cations from wastewaters. However, its direct use in a separation / filtration system is very difficult mainly because of its fine particle size. But the coating with a thin layer of iron hydroxide (as ferrihydrite) onto HCl-activated brick pellets has proved to enhance significantly adsorption capacity for divalent metals when compared to raw brick [20-21]. It is well known that the complexity of naturally occurring ferrihydrite is due to the presence of inorganic impurities including: silicon and aluminum that can affect its composition, crystallinity, solubility and even its thermodynamic stability. Micro-analyses permitted us to detect the presence of Al and Si in brick ferrihydrite (Allahdin et al. unpublished works), suggesting structural incorporation to surface complexation and/or surface precipitation as, *e.g.*: strong-binding ligands from brick clays being suspected to be associated with the surface of ferrihydrite particles.

In this work, modified brick was used as a cations adsorbent in deionized water and the common metallic pollutants Cd^{++}, Cu^{++}, Zn^{++} and Pb^{++} were selected as adsorbates because of their bad effect on aquatic media. Adsorption properties of other cations were also examined in the present work only for data comparison: Ca^{2+}, Fe^{2+}, Mg^{2+}, Mn^{2+}, Sr^{2+}. It should be noted that: (i) the adsorption process was examined here only in single-metal system (and not in multi-metals system); and (ii) data on desorption isotherms and desorption rate were not reported here (although numerous works are under way in our lab in the role of added inert electrolytes on the kinetic rate, the importance of bleach in the regeneration process of brick, and the implication of electrostatic forces induced by H^+ and/ or OH^- ions as potential determining ions on the adsorption capacity of brick). Langmuir and Freundlich isotherms were used to assess the equilibrium data. The adsorption kinetics was studied at varying temperatures based on the pseudo-first and pseudo-second-order kinetics models. The implication of acidic (hydrolysis) properties of divalent cations in water on the adsorption process was studied.

2. MATERIALS AND METHODS

2.1 Adsorbent Preparation and General Characteristics

The raw brick used in this study was obtained from Bangui region in the Central African Republic. Previously, X-ray diffraction and chemical analysis were performed on this material: ∼ 61 wt % quartz; ∼ 21 wt % metakaolinite; 3-4 wt % illite; ≤ 4 wt % iron oxides / hydroxides; and ≤ 2 wt % feldspar + mica + biotite [17]. Before use, several physical / chemical treatments were carried out on the raw brick [17,18]. Briefly: (i) it was broken into grains and sieved with sizes ranging from 0.7 to 1.0 mm; (ii) the resulting particles were leached with a 6M HCl solution at 90°C for 3 hours; and (iii) finally a deposition of FeOOH onto HCl - treated brick was made by precipitation of iron(III) with a NaOH solution up to attain pH ~ 7. After these chemical treatments, resulting particles were sized again with 0.7-1.0 sizes, and some of their physical characteristics were assessed: surface area, 70 m^2/g; pore volume, 0.21 cm^3/g; and density 0.845 ± 0.027 g/dm^3.

Chemical and spectroscopic analyses were previously performed on brick samples [18, 21]. Briefly, it was found that: (i) after acid leaching of raw brick at 90°C, Al content decreased in the porous material and FT-IR spectroscopy permitted us to detect Brönsted (protonic) and Lewis (aprotonic) acid sites at the surfaces of grains [18]; and (ii) after FeOOH deposition ^{23}Na MAS NMR revealed the involvement of sorbed Na^+ ions to form outer-sphere complexes with the active brick sites, and ^{1}H MAS NMR further showed only a broad line shape which was caused by dipole-dipole interactions between brick protons (when water molecules diffused on the brick surface and visited the various types of hydroxyl groups: Si-OH, Al-OH, and Fe-OH) [21]. It is worth noting that the interaction of Me^{2+} ions with brick led to a chemical combination "Me^{2+}--brick" with several 1H MAS NMR resonances which were ascribed to protons of silanols and aluminols in the brick [21].

2.2 Chemicals

All chemicals used in the study were analytical grades. Sodium hydroxide and hydrochloride acid were supplied by DISLAB (France). The following salts: $Cd(NO_3)_2 \cdot 4H_2O$, $Fe(NO_3)_3 \cdot H_2O$, and $Pb(NO_3)_2$ were purchased from Prolabo. $Cu(NO_3)_2 \cdot 3H_2O$ was obtained from Scharlau, $Ca(NO_3)_2 \cdot 4H_2O$, $Mg(NO_3)_2 \cdot 6H_2O$, $Sr(NO_3)_2$, $FeCl_2 \cdot 4H_20$ and $Mn(NO_3)_2 \cdot 4H_2O$ were purchased from Merck, and $Zn(NO_3)_2 \cdot 6H_2O$ from Fluka. For kinetics experiments, divalent - metal salts were first diluted in Milli-Q water to obtain a $7.16x10^{-3}$ mole-per-liter solution (in the case of iron, this concentration corresponded to 400 mg per liter); The stock solutions of cationic metals were second diluted ten-fold to obtain an experimental-solution concentration of $7.16x10^{-4}$mol-per-liter.

2.3 Isotherm Studies

To study the adsorption behavior of the metal ions on modified brick, the experiments for adsorption isotherms were performed at room temperature and under constant stirring condition. Isotherm studies on divalent cations (Ca^{2+}, Cd^{2+}, Cu^{2+}, Mg^{2+}, Pb^{2+} and Zn^{2+}) adsorption onto Bangui brick were carried out on brick grains with 0.7 -1.0 mm sizes. These experiments were performed in ten 100mL-flasks –each one containing 1g of brick pellets— in which were added 50 mL of a divalent-cation solution with a concentration ranging from $1.15x10^{-4}$ to $7.80x10^{-4}$mol/L. These flasks were placed on a mechanical (orbital) shaker (Model: IKA Labortechnik KS 250 basic) and gently shaked at a speed of 120 rpm. Adsorption-isotherm experiments lasted one night although a reaction time of 4 hours at a temperature of 17°C ± 1°C was sufficient for the system to attain thermodynamic equilibrium. Afterwards, suspensions were filtered and the recovered solution was analyzed to determine cation concentrations using an ICP-AES (Inductively Coupled Plasma Atomic Emission Spectroscopy; Model: Varian Pro axial view) spectrometer. The quantity of solute adsorbed onto brick pellets, noted Qe (in mg/g), was assessed from the difference between the initial and the equilibrium contents of cationic ions in the liquid phase. It should be noted that all these experiments were at least triplicated and data were averaged.

2.4 Kinetic Studies

For each kinetic experiment, 1 g of modified brick pellets (with average diameters varying from 0.7 to 1.0 mm) was added to 100 mL of the diluted metal solution ($7.16x10^{-4}$mol/L) at a fixed temperature. This suspension was continuously and gingerly mixed with a propeller stirring and pH was measured during the process. 1 mL of the supernatant (which was filtered through a 0.45 µm pore diameter cellulose nitrate filter) was collected at various time intervals from 0 to 60 minutes and analyzed for the determination of metal level by ICP-AES. The reproducibility of concentration measurements was ensured by repeating three times the same experiments under identical experiment conditions. This procedure permitted us to determine average values of metal content in the reaction solution, and standard deviations of these analyses were evaluated to be within ± 3%. The Me(II) adsorption capacity of brick was calculated by using the following equation: Qe = (Co – Ce)V/m, where Qe represents the adsorption capacity of divalent metal on FeOOH-coated brick (in mg/g); Co is the initial content of Me^{2+} ions in the cell (in mg/L); Ce represents the equilibrium solute concentration (in mg/L); and m and V correspond to the mass of brick used (g) and the volume of Me(II) solution used (L), respectively. At this metal concentration ($7.16x10_{-4}$mol/L), Fe^{2+} ions remained at oxidation state II under our physicochemical (O_2, natural potential Eh and pH) conditions, according pε – pH diagrams for iron-water system [22].

3. RESULTS AND DISCUSSION

3.1 Adsorption Isotherms

In order to relate the adsorbate concentration in the bulk solution with the adsorbed content present at the adsorbent surface, several adsorption equations were proposed in the literature [23-33]. Two of them were selected for this work: Langmuir and Freundlich ones [23,25,33]. The Langmuir –isotherm model was *first* applied to our systems by assuming that the observed adsorption occurred onto homogeneous brick surfaces with a specific number of equivalent sites. For fitting of the experimental data, a linear form of Langmuir model was used [25,33]:

$$\frac{1}{Qe} = \frac{1}{Q_{\max}} + \frac{1}{bQ_{\max}Ce} \tag{1}$$

where Ce is the concentration of metal ions at equilibrium in the solution (mg/L); Q_e represents the amount of divalent metals adsorbed at brick surfaces (mg/g); Q_{max} corresponds to the amount of metal ions at complete monolayer coverage (mg/g), and b is Langmuir constant which depends upon the adsorption energy. The parameters, b and Q_{max}, were calculated from the intercepts and slopes of the Langmuir plots of $1/Q_e$ against $1/C_e$ that were drawn for the different studied cations (see Fig. 1 and Table 1).

The Freundlich-isotherm model was *second* applied to our systems by assuming, in this case, the existence of several types of adsorption sites on heterogeneous brick surfaces. This model could be described by the following equation [23,33]:

$$LogQe = LogK_F + (\frac{1}{n})LogCe \tag{2}$$

Where K_F is the sorption capacity constant (mg/g); and n is the sorption intensity constant K_F and n were calculated from the intercepts and slopes of the Freundlich plots of $LogQe$ against $LogCe$ (see Fig. 1 and Table 1).

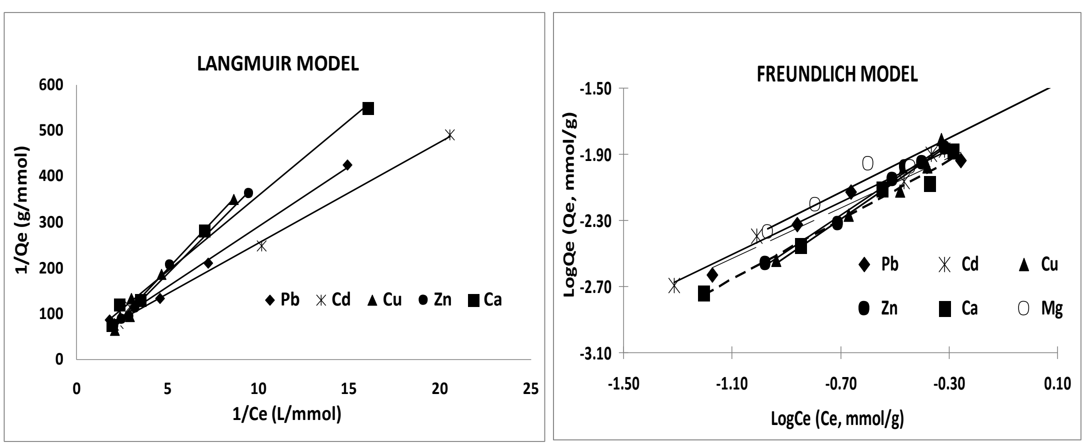

Fig. 1. Adsorption isotherms of some divalent cations on modified brick fitted using Langmuir and Freundlich models at room temperature.

Table 1. Langmuir and Freundlich constants for the adsorption of some divalent cations by modified brick in water at room temperature.

	Q_{max} *µmol/g*	b *L/mg*	K_F *mg/g*	n	R_L
Cu^{2+}	100.5	0.0029	0.1781	0.8994	0.86-0.94
Zn^{2+}	79.5	0.0063	0.1879	0.9158	0.83-0.95
Pb^{2+}	37.0	0.0050	0.3198	1.3098	0.55-0.89
Ca^{2+}	27.1	0.0286	0.2229	1.1173	0.60-0.92
Cd^{2+}	24.0	0.0815	0.5521	1.6804	0.41-0.85
Mg^{2+}	22.1	0.0935	0.2707	1.2143	0.45-0.75

Overall, our findings revealed that our experimental data fitted Langmuir isotherm better than Freundlich one, with a regression coefficient $R^2 > 0.997$. Therefore, this adsorption process acted more as a monolayer adsorption on the surface of modified brick under our applied experimental conditions. The maximum adsorption capacity, Q_{max}, from the Langmuir isotherm was found to decrease in the following order: Cu(II)>Zn(II)>Pb(II)>Ca(II)>Cd(II)>Mg(II). Comparable adsorption-capacity values were previously found for iron(II): 12-28.6 µmol/g [18,19]. Variable physico-chemical phenomena were involved in these systems because of different hydrolysis characteristics of these cations, and thereby these complicated any interpretation of this order.

To further predict whether or not the study adsorption was favorable, a dimensionless separation factor — which was associated with the Langmuir isotherm and called equilibrium parameter (R_L)— was calculated from the following equation [34]:

$$R_L = \frac{1}{1 + bCo} \tag{3}$$

where Co represents the initial concentration of divalent cations in the medium (in mg/L). The value of R_L permitted us to show whether the adsorption process was: irreversible (R_L =0); favorable (R_L<1); linear (R_L =1); or unfavorable (R_L>1) [34]. Indeed, the fact that all the R_L values obtained in this work for the adsorption of cationic entities on modified brick were in the range of 0.41 – 0.95 (see Table 1), implied that this adsorption process was favorable. In addition, the n values for the different cations were found to be higher than 1, indicating a (moderately) favorable adsorption mechanism. A comparison of the maximum capacities of these cations on ferrihydrite - coated (pre-activated) brick with those on other iron-bearing minerals –which were reported as promising metals adsorbents in the literature— was made in the present work (see Table 2). It should however be noted that because of variation in parameters and experimental conditions applied, direct comparison with other published data ought to be considered as tentative. It could nevertheless be noticed that the material used in this work possessed adsorption characteristics somewhat close enough to those observed for different iron-bearing adsorbents cited in the literature (see Table 2). Moreover, in our investigations the Q_{max} values were found to be strongly dependent upon the content of ferrihydrite coating the brick surface. This, when calculating the adsorption capacity by referring directly to the amount of ferrihydrite deposited onto brick pellets, Q_{max} could theoretically reach values up to 100 times higher than those obtained in this work. This implied that, if pre-activated brick was sufficiently impregnated with ferrihydrite, the resulting material should possess an additional potential for practical application in heavy-metal removals from wastewaters.

Table 2. Comparison of adsorption performance of ferrihydrite-coated brick for divalent-cations removals with those observed for other iron oxide-bearing materials

Coating	Support material	Adsorbed divalent metals	Removal performance mmol/g	Refs.
Ironoxide	Alumina	Pb	Pb (0.14)	[35]
	Bentonite	Pb	Pb (0.107)	[36]
	Sand	Cu ; Pb	Cu (0.004) ; Pb(0.006)	[37]
	Sand (ferruginous)	Cu	Cu (0.032)	[38]
	Sewage sludge	Cu ; Cd ; Pb	Cu (0.27); Cd (0.13); Pb (0.21)	[39]
	Waste silica gel	Cu ; Cd ; Pb	Cu (0.053); Cd (0.038); Pb (0.039)	[40]
	Sepiolite	Pb	Pb (0.366)	[41]
Goethite	Sand	Cd; Pb	Cd (0.006); Pb (<0.001)	[42]
	Sand (quartz)	Cd	Cd (0.002)	[43]
		Cu; Pb	Cu (0.004); Pb (0.006)	[44]
	Clinoptilolite	Cu; Zn	Cu (0.5); Zn (0.2)	[45]
Hydrated ferric oxide	Polyacrylamide	Cd; Pb	Cd (1.309); Pb (1.020)	[46]
Fe, Mg hydr(oxides)	Bentonite	Pb	Pb (0.463)	[47]
Ferrihydrite	(Pre-activated) brick (*)	Fe(II) in Bangui ground waters (§)	Fe (0.015)	[20]
	(Pre-activated) brick (*)	Ca; Cd; Cu; Mg; Pb; Zn	Ca (0.037); Cd (0.024); Cu (0.100); Mg (0.022); Pb (0.037); Zn (0.079)	This work

(*) Raw brick made in Bangui region (Central African Republic) was first pre-activated with a 6M-HCl solution at 90°C for 3 hours (and, second impregnated with ferrihydrite by Fe(III) precipitation with NaOH to pH 7).
(§) Modified brick was tested in soluble iron(II) removals from Bangui ground waters.

3.2 Adsorption Kinetics

Adsorption-kinetics studies were useful in assessing the metal - ions uptake rate and in gaining information about the study mechanism [47]. To investigate the kinetics of the heterogeneous reaction between cationic entity and brick, it was preliminarily important to monitor how fast the reaction took place under our experimental conditions.

Concentration removal of metal ions from solution at different temperatures and under constant stirring condition was determined by ICP-AES. For instance, Fig. 2 shows how the concentration of Pb(II) varied with time during several experiments performed at temperatures ranging from 20 - 35°C.

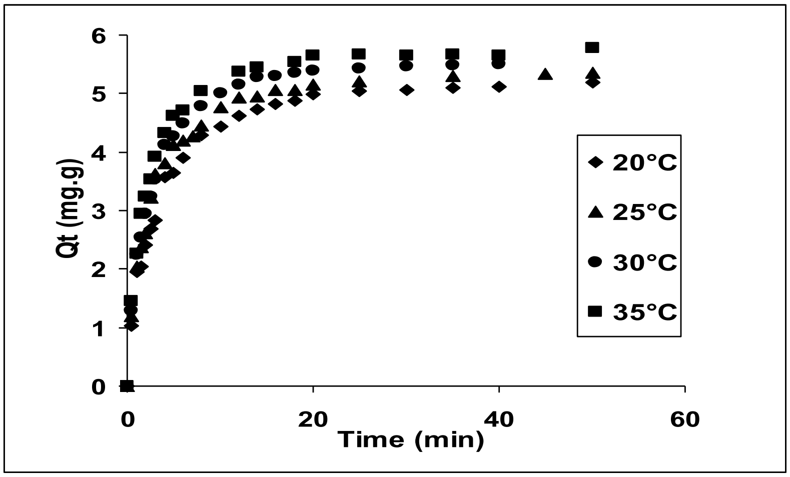

Fig. 2. Effect of temperature on the adsorption kinetics of Pb^{2+} ions by modified brick grains.

Brick = 4g, [Cation] = 7.16 x10^{-4}mol/L, Volume = 100 mL.

Overall, it was found that: (i) the adsorption process was quite rapid in the first 20 min and about 1 hour was necessary to reach an equilibrium state (Fig. 2); and (ii) an increase in the temperature resulted in increasing Pb(II) adsorption rate (Fig. 2), thus revealing the process to be endothermic. This will be confirmed and detailed in section 3.3. Similar trends were found for the removal of the other cations studied here (***i.e.***, Cd^{2+}, Cu^{2+}, Mg^{2+}, Sr^{2+}, and Zn^{2+}) from water by modified brick in a similar temperature range. Two kinetics models –namely pseudo-first-order and pseudo-second-order— were used in this work. For these kinetics studies, we had taken in account James and Healy's suggestions [10], *i.e*: adsorption cannot depend upon the appearance of a specific ionic species such as the first or other hydrolysis product and even specific polynuclear complexes. In this assumption, the pseudo-first-order kinetic rate expression (Lagergren equation) could be given as [48, 49]:

$$Ln(Qe - Qt) = Ln(Qe) - k_1 t \tag{4}$$

where *Qe* and *Qt* (mg/g) represent the amounts of divalent cation (Cd^{2+}, Cu^{2+}, Mg^{2+}, Pb^{2+}, Sr^{2+} and Zn^{2+}) adsorbed per unit weight of brick at equilibrium and time t (min), respectively; and K_1 (1/min) is the rate constant of pseudo-first-order sorption. The pseudo-second-order kinetics rate expression (Ho equation) could be given as [48,50]:

$$\frac{t}{Qt} = \frac{1}{k_2 Qe^2} + \frac{t}{Qe} \tag{5}$$

Where k_2 (g/(mg.min) is the rate constant of pseudo-second-order adsorption. The plots of *Ln(Qe –Qt)* versus *t* and *t/Qt* versus t gave straight lines (see Fig. 3). The values of k_1, k_2, and *Qe* were obtained from the intercepts and slopes of these straight lines.

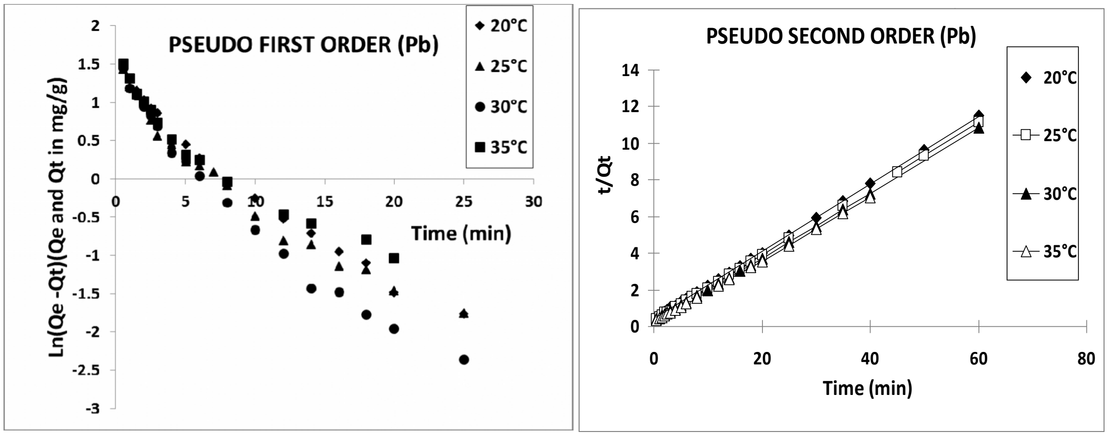

Fig. 3. Pseudo-first order and pseudo-second order kinetic plots, Ln(Qe – Qt) *vs* t and t/Qt*vs* t, for the adsorption of divalent cations onto modified brick grains at 298°K.
Qe and Qt(mg/g) are the amounts of adsorbed cations at equilibrium and time t (min), respectively.

Kinetics parameters calculated from linear plots of both models and correlation coefficient values are given in Table 3. It was noticed that the adsorption kinetics data fitted both models very well ($R^2 > 0.9$). However, good linearity of the Lagergren pseudo-first-order plot observed for these divalent cations was no assurance that the process would follow first-order kinetics. Indeed, adsorption data were found to fit better the pseudo-second-order model judging by higher R^2 values ($R^2 > 0.998$; see Table 3). Furthermore, as reported in Table 3 experimental and theoretical *Qe* values of the second-order model revealed better consistencies, when compared to the first-order model. Therefore, these findings implied that the adsorption process adhered more to the pseudo-second-order kinetics. Such a model then assumed that one divalent cation (Me^{2+}) was adsorbed onto two sorption sites (noted 2A) on the brick surface according to [19]:

$$2\ A^-_{(brick)} + Me^{2+}_{(solution)} \rightarrow A_2Me_{(brick)}$$

Table 3. Pseudo-first-order and pseudo-second-order kinetics parameters measured at different temperatures for the adsorption of some divalent cations onto modified brick in Milli-Q water. pH_i is the 'initial' pH value measured at the beginning of the reaction

			Pseudo-first order kinetics				Pseudo-second orderkinetics			
	T°K	pH_i	Q_e *exp.* *(μmol/g)*	Q_e *cal.* *μmol/g)*	k_1 *(1/min)*	R^2	Q_e *cal.* *(μmol/g)*	k_2 *(g/(mg.min))*	k_2 *(g/(mM. min))*	R^2
Pb^{2+}	293	5.3	25.17	12.71	0.097	0.9507	26.1	0.085	17.637	0.9998
Cu^{2+}	294.2	5.51	21.72	16.43	0.19	0.9624	22.53	0.361	*22.947*	0.9992
Cd^{2+}	293.2	6.9	20.88	14.02	0.204	0.9926	21.46	0.255	28.608	0.9996
Zn^{2+}	295.1	6.49	17.27	10.26	0.16	0.9549	17.4	0.529	34.593	0.9993
Mg^{2+}	293.2	8.09	14.59	7.37	0.172	0.9437	14.97	2.073	50.379	0.9996
Sr^{2+}	294.8	8.69	9.91	9.5	0.3	0.9841	10.38	0.645	56.489	0.9976
Pb^{2+}	298	5.31	25.95	11.39	0.099	0.9532	26.65	0.107	22.233	0.9998
Cu^{2+}	298.2	5.47	24.07	15.65	0.136	0.9776	25.3	0.255	16.204	0.9993
Cd^{2+}	298.2	6.87	19.76	11.09	0.2	0.9612	20.14	0.286	32.111	0.9997
Zn^{2+}	298.5	6.5	16.3	12.86	0.174	0.9966	16.94	0.689	45.066	0.9993
Mg^{2+}	298.2	7.94	14.33	8.49	0.239	0.9084	14.84	2.211	53.743	0.9985

Table 3 Continue……….

Sr^{2+}	300	8.58	10.7	7.22	0.262	0.9683	11.05	0.833	73.023	0.9989
Pb^{2+}	303	5.67	26.68	12.23	0.127	0.9483	27.41	0.119	24.719	0.9997
Cu^{2+}	303.2	5.42	22.23	15.76	0.218	0.9349	22.55	0.5	31.741	0.9991
Cd^{2+}	303.2	6.81	21.23	12.65	0.171	0.9694	21.26	0.319	35.904	0.9994
Zn^{2+}	303.3	6.53	16.81	11.99	0.197	0.9754	17.27	0.731	47.767	0.9996
Mg^{2+}	303.2	7.92	13.78	5.67	0.113	0.9052	13.71	3.006	73.056	0.999
Sr^{2+}	303.2	8.55	9.56	9.98	0.332	0.9891	11.25	0.759	66.539	0.9981
Pb^{2+}	308	5.71	27.33	15.86	0.122	0.9341	28.63	0.131	27.102	0.999
Cu^{2+}	308.2	5.39	21.52	11.33	0.11	0.8997	20.96	0.438	27.808	0.9974
Cd^{2+}	308.2	6.78	21.53	11.75	0.201	0.9669	22.11	0.356	39.996	0.9997
Zn^{2+}	308.2	6.57	18.21	8.74	0.205	0.959	18.64	0.826	53.997	0.9997
Mg^{2+}	308.2	7.87	13.67	11.01	0.688	0.8798	13.67	3.442	83.648	0.9996
Sr^{2+}	308.3	8.47	9.85	9.64	0.381	0.9992	10.15	1.001	87.734	0.9987

3.3 Adsorption Activation Energy Kinetics

In the above section, the pseudo second-order model was identified as the best kinetic model for mathematical treatment of our experimental data. In the present section the rate constant, k_2, of the pseudo-second order model was used to evaluate the activation energy of the adsorption process by using Arrhenius equation:

$$Ln(k_2) = Ln(A) - \frac{Ea}{RT} \tag{6}$$

where A and Ea are the Arrhenius factor and the activation energy, respectively; and R and T are the ideal gas constant (8.314J/(mol.K)) and the absolute temperature (°K), respectively. By plotting $\ln(k_2)$ versus 1/T (for instance for Pb(II); see Fig. 4) and from the slopes and intercepts, E_a values for the different divalent-cations adsorption reactions could be attained. The positive values of Ea suggested that increase in temperature favored the adsorption process. Consequently, the study mechanism was an endothermic one in nature. To know whether the adsorption process was mainly physical or chemical one, it was previously suggested that activation energies should range from ~ 5 to ~ 40 kJ/mol for physisorption reactions and from ~ 40 to ~ 800 kJ/mol for chemisorption ones [51-53]. All the Ea values obtained in this study were found to be < 40 kJ/mol (see Table 4), indicating that studied Me^{2+}-ions adsorption reactions possessed low potential barriers and were dominantly assigned to a physisorption phenomenon [51,52,54].

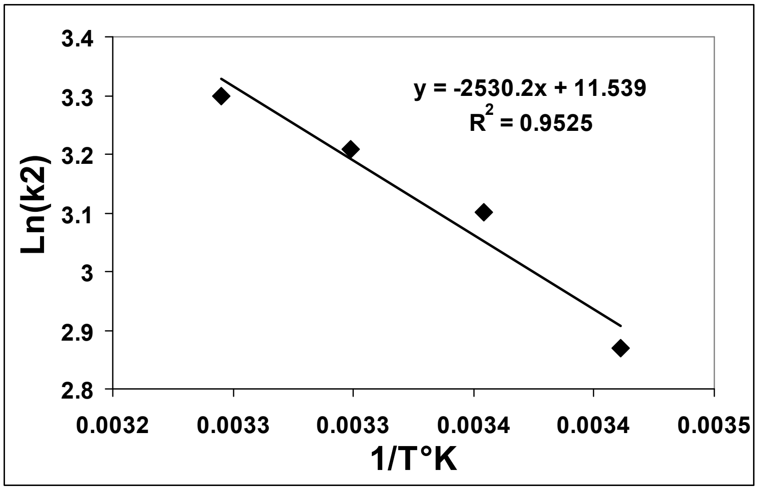

Fig. 4. Arrhenius plot, Ln(k_2) *vs* 1/T, for the adsorption of Pb^{2+} ions on modified brick grains at 298°K.

k_2 is expressed in g/(mM.min).

Physisorption needs little energy to perform, whereas chemisorption demands much higher energies. Moreover, brick was negatively charged at the medium pH and thereby should attract positive ions at its surface [55]. Therefore, owing to the implications of electrostatic forces, physisorption should be predominant in this adsorption process, as pointed out by Li and his coworkers [55]. To know whether the adsorption process involved activated (intermediate) complexes, the enthalpy (ΔHa) and the entropy (ΔSa) of activation were assessed using Eyring equation:

$$Ln\left(\frac{k_2}{T}\right) = Ln\left(\frac{k_B}{h}\right) - \frac{\Delta Ha}{RT} + \frac{\Delta Sa}{R} \tag{7}$$

Table 4. Thermodynamic parameters for the adsorption kinetics of divalent cations onto modified brick

	Ea	**Thermodynamic parameters of pseudo-second order kinetics**					
		ΔHa	**ΔSa**	**ΔGa $_{(293°K)}$**	**ΔGa $_{(298°K)}$**	**ΔGa $_{(303°K)}$**	**ΔGa $_{(308°K)}$**
	kJ/mol	***kJ/mol***	***J(mol.K)***	***kJ/mol***	***kJ/mol***	***kJ/mol***	***kJ/mol***
Pb	20.997	18.510	-178.40	70.781	71.673	72.565	73.457
Cu	20.919	18.416	-168.53	67.795	68.638	69.480	70.323
Cd	16.769	14.271	-184.11	68.214	69.135	70.056	70.976
Zn	23.281	20.768	-155.83	66.426	67.205	67.984	68.763
Mg	27.588	25.108	-153.46	70.072	70.839	71.606	72.373
Sr	21.522	19.017	-160.45	66.029	66.831	67.633	68.436

Where k_B is Boltzmann constant; *h* is Planck constant; and the other parameters are already defined above. The plots of $Ln(k_2/T)$ versus 1/T were found to be straight lines (for instance for Pb: see Fig. 5), and their slopes and intercepts were used to calculate ΔHa and ΔSa (see Table 4). Furthermore, the Gibbs free energy of activation, ΔGa, could be expressed in terms of enthalpy and entropy of activation as follows:

$$\Delta Ga = \Delta Ha - T\Delta Sa \quad (8)$$

The ΔGa values obtained for the different adsorption reactions between divalent cations and brick grains varied from *ca* +60 to +71 kJ/mol at 298°K (see Table 4). Note that the free energy of activation can be obtained from the rate constant, (k) through the Activated Complex Theory equation (also known as Eyring-Polanyi equation): $k = CT\exp(-\Delta Ga/RT)$, where C is a constant. And like this work, positive ΔGa values were found either for metal adsorptions [56] or geochemical transformations [57].

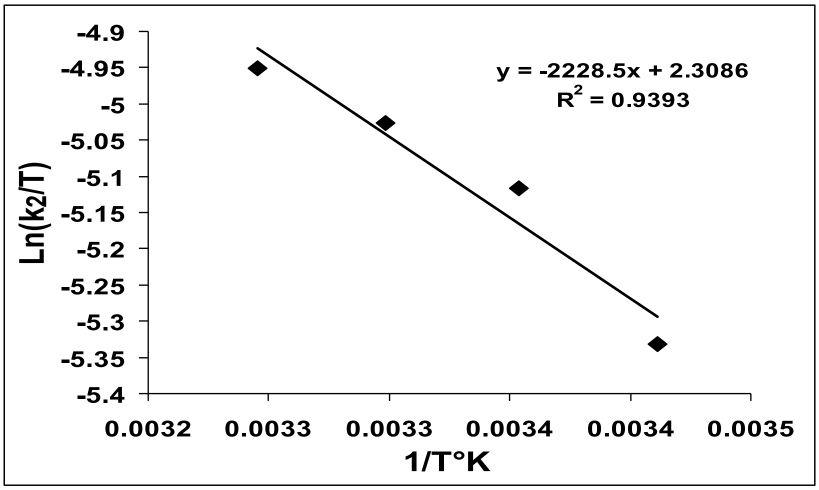

Fig. 5. Eyring plot, $Ln(k_2/T)$ *vs* 1/T, for the adsorption of Pb^{2+} ions on modified brick grains at 298°K.
*k_2 is expressed in the International System***.**

The positive values of ΔHa (ranging from *ca.* +14 to +21 kJ/mol; see Table 4) showed that this process consumed energy and thereby was endothermic. As for activation entropy, their negative values (ranging from *ca.* -153 to -178 J/(mol.K); see Table 4) suggested two features: (i) partial orders occurred at the beginning of the kinetic step due to electrostatic attraction phenomena [55], before any structural (chemical) changes at the adsorbent /ferrihydrite surface; and (ii) schematically metal ion was adsorbed onto brick surface through the formation of an activated (intermediate) complex according to an associative mechanism [58,59,60]. It is worth noting that these thermodynamic (activation) parameters revealing the relevance in the energetics of the kinetic heterogeneous process studied, are in the range of those reported in the literature concerning kinetics of metal adsorption on adsorbents like activated carbon [56] and even of various geochemical transformations [57].

3.4 Interpretation of the Adsorption Process

Negatively and positively charged sites could appear at the brick surface through deprotonation and protonation of -OH groups at proportions that were dependent upon the medium pH. The amphoteric edge hydroxyl groups (denoted here: ≡S-OH) then accounted for possible chemical equilibria showing partial and specific adsorptions of metallic cation onto modified brick grains as follows:

$$(\equiv S\text{-}OH) + Me^{2+} \leftrightarrow (\equiv S\text{-}O)Me^{+} + H^{+} \quad (9)$$

and/or

$$2(\equiv S\text{-}OH) + Me^{2+} \leftrightarrow (\equiv S\text{-}O)_2Me + 2\,H^+ \quad (10)$$

Moreover, the interaction of metallic cations with ferrihydrite - coated brick resulted more in inner-sphere complexes [21]. Furthermore, as observed for kaolinite [61] (which also contains ≡Si-OH and ≡Al-OH groups), the most probable sites for the forming of inner-sphere complexes with Me^{2+} ions were negatively charged edge sites, $\equiv SO^-$.. The Me^{2+}-ions removal from the solution by modified brick resulted in a decrease of solution pH [20,21], however, this increasing of H^+ concentration was largely insufficient to achieve molecular and electric balances and Na^+ ions ought to be taken into account in the process [20,21]. On the other hand, as shown in Fig. 6 the pseudo-second-order kinetics rate, k_2, was dependent on the hydrolysis characteristics of divalent cations as [61-62]:

$$Me^{2+} + H_2O \leftrightarrow Me(OH)^+ + H^+. \quad (11).$$

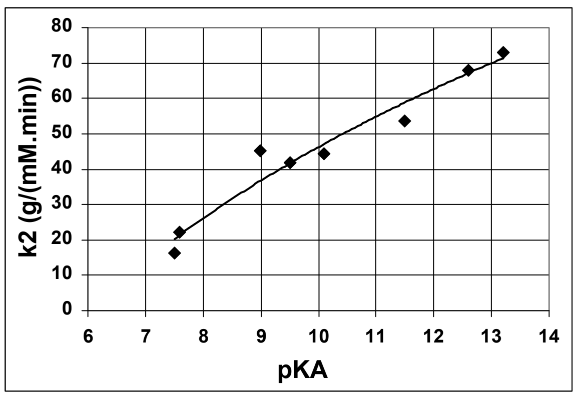

Fig. 6. pK_A-dependence of the pseudo-second order kinetic rate (k_2).
K_A represents the first hydrolysis (acidity) constant of divalent cation [61-63].

All these observations indicated clearly that more the difference between solution pH and pH_{PZC} (the pH value at the point of zero charge, PZC: 3.2) was high and more electrostatic forces increased and facilitated the process in due course. This explained the decrease observed for k_2 values: from 73.0 for Sr^{2+} to 22.2 g/(mM.min) for Pb^{2+} (see Table 3). Deprotonated functional groups (which were previously generated during the preparation / activation of modified brick through Fe(III) precipitation with NaOH), were found to be more beneficial for the adsorption process. Indeed, this chemical treatment led to: (i) few H^+ competing with Me(II) for the adsorption sites of brick; and (ii) more Na^+ ions exchanging predominantly with Me(II) at the water-brick interface.. A general mechanism was then proposed:

$$2(\equiv S\text{-}OH) + Me^{2+} \leftrightarrow (\equiv S\text{-}O)_2Me + 2\,H^+ \quad (12)$$

$$2(\equiv S\text{-}ONa\ ) + Me^{2+} \leftrightarrow (\equiv S\text{-}O)_2Me + 2\,Na^+ \quad (13)$$

The metal binding constants, $K_{(\equiv SOMe)}$ relative to equation 9, which were reported previously for kaolinite [61] (see Table 5), were used in the present work because brick hydroxylation generated hydroxyl groups at the brick-metakaolinite surface with chemical characteristics similar to those observed at the kaolinite surface. The surface binding constant, log[(K($_{\equiv SOMe}$)], was plotted against the adsorption capacity, Qe (Fig. 7).

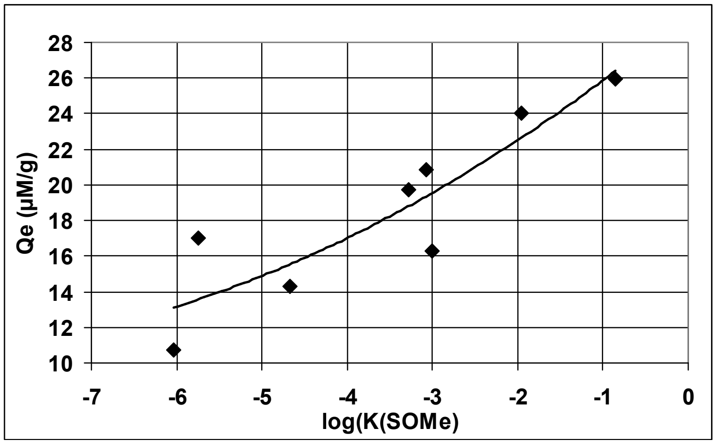

Fig. 7. Correlation of surface complexation constants, K($_{\equiv SOMe}$)*, of eight cations adsorbed onto hydroxyl groups from brick metakaolinite (after its modification) with the amount of adsorbed cation, Qe, at equilibrium.
(*) Constants for complexation between metals and kaolinite [61].

A relationship was found between this binding constant and Qe, revealing an implication of hydroxyl groups of metakaolinite in addition to the –OH and/or –O^-Na^+ functions of brick ferrihydrite. As a whole, the adsorption affinity of the studied eight elements onto ≡S-OH sites in modified brick had the following order: Pb> Cu > Cd ≈ Mn ≈ Zn > Mg >Ca> Sr.

To summarize, the magnitude of Qe was dependent upon complexing interactions between ≡S-O^- and Me^{2+}, while the kinetic constant was related to electrostatic attractions between charged sites on the brick and ions in water. Therefore, Qe varied with the stability constant of the generated complex, and k_2 was influenced by H^+ and OH^- (*i.e.*, the pH of the studied suspension) as potential-determining ions by regulating proportions of negative and positive charges at the brick surface.

Table 5. First hydrolysis constants, pKA, of divalent cations and their surface complexation constants, $K_{(\equiv SOMe)}$, when adsorbed onto hydroxyl groups from brick metakaolinite (*Qe represents the amount of adsorbed cations on the equilibrium state*)

Cations	Qe(µmol/g)	pK_A(*)	log[(K($_{\equiv SOMe}$)]$^{(§)}$
Ca^{2+}	17.04	12.6	~-5.75
Cd^{2+}	19.76	10.097	-3.28
Cu^{2+}	24.06	7.497	-1.96
Mg^{2+}	14.33	11.5	~-4.67
Mn^{2+}	20.84	9.5	~-3.07
Pb^{2+}	25.95	7.597	-0.85
Sr^{2+}	10.70	13.2	~-6.03
Zn^{2+}	16.30	8.997	-3.01

(*) First hydrolysis constants from refs [61-63]. (§) Constants for complexation between metals and kaolinite [61].

4. CONCLUSION

In this study, a successful ferrihydrite-coated (pre-activated) brick filter was developed for the removal metallic cations from water. This adsorption process was found to be better fitted by Langmuir model. The amount of divalent cations at complete monolayer coverage, Q_{max} was assessed by Langmuir isotherms and followed a descending sequence (in µmol/g):

$$Cu^{2+} (100.5 > Zn^{2+} (79.5) > Pb^{2+} (37.0) > Ca^{2+} (27.1) > Cd^{2+} (24.0) > Mg^{2+} (22.1).$$

As for the kinetic aspects of the adsorption reaction, experimental data were described better by the pseudo-second order adsorption kinetic rate model. The corresponding rate constant for this adsorption was found to decrease in the following order (k_2 at ~ 298°K expressed in g/(mM.min)): Sr (73.02); Zn (45.06); Fe (44.39); Cd (33.7); Pb (22.23); Cu (16.20). The activation parameters of the kinetics process enabled us to predict how the adsorption of divalent cations varied with temperature changes: (i) the Gibbs free energy of activation and the activation enthalpy revealed an endothermic performance for the adsorption of Me^{2+} ions onto modified brick; and (ii) the activation entropy reflected the decrease of randomness at the solid-solute interface mainly as a consequence of electrostatic attraction followed by an intermediate hydroxyl complexation in the ferrihydrite phase: such a combination was thought to form with time inner-sphere complexes on negatively charged sites of the brick.

The differences observed in kinetic rate constants towards the sorbent surface were related mostly to the acidic (hydrolysis) properties of these divalent cations in water (pK_A) and the pH-dependence of the brick-surface charges. This suggested that H^+ and OH^- are potential - determining ions in the electrokinetic behavior of ions adsorption onto solids by generating electrostatic forces at the brick-water interface, as already suggested by Wiese and his coworkers [64]. Moreover, the amount of adsorbed cations at the equilibrium state (Qe) – which was evaluated from kinetic studies— followed the decreasing order: Pb> Cu ~ Cd > Zn > Mg.. This order resulted in the extent of complexation between active brick sites and cations in aqueous solution. This hypothesis was sustained by a relationship between Qe and the surface binding constant, $K_{(\equiv SOMe)}$ in kaolinite.

ACKNOWLEDGMENTS

This work is partly funded by the “Agence de l’Eau Artois-Picardie,” the “Region Nord Pas-de-Calais,” and the “ConseilGénéral du Nord,” The study is part of Oscar Allahdin’s thesis which is currently underway, and results from the cooperation between the University of Lille1 (France) and the University of Bangui (Central African Republic). This collaboration and the Grant-in Aid to Mr. O. Allahdin for his scientific research are financially supported by the Embassy of France to Bangui.

COMPETING INTERESTS

Authors have declared that no competing interests exist.

REFERENCES

1. Ali H, Khan E, Sajad A. Phytoremediation of heavy metals -Concepts and applications: A review, Chemosphere. 2013;91:869-881. And references therein.
2. Fu F, Wang Q. Removal of heavy metal ions from wastewaters: A review, J. Environ. Manage. 2011;92:407-418.
3. Pérez-González A, Urtiaga AM, Ibáñez R, Ortiz I. State of the art and review on the treatment technologies of water reverse osmosis concentrates. Water Res. 2012;46:267-283.
4. Kurniawan TA, Chan GYS, Lo WH, Babel S. Physico-chemical treatment techniques for wastewater laden with heavy metals, Chem. Eng. J. 2006;118:83-98.
5. Loo SL, Fane AG, Krantz WB, Lim TT. Emergency water supply: A review of potential technologies and selection criteria. 2012;46:3125-3151.
6. Al Abdugader H, Kochkodan V, Hilal N. Hybrid ion exchange— Pressure driven membrane processes in water treatment: A review, Sep. Purif. Technol. 2013;116:253-264.
7. Norton-Brandăo D, Scherrenberg SM, van Lier JB. Reclamation of used urban waters for irrigation purposes— A review of treatment technologies. J. Environ. Manage. 2013;122:85-98.
8. Chong MN, Jin B, Chow CWK, Saint C. Recent developments in photocatalytic water treatment technology: A review, Water Res. 2010;44:2997-3027.
9. Babel S, Kurniawan TA. Low-cost adsorbents for heavy metals uptake from contaminated water: A review, J. Hazard. Mater. 2003;B97:219-243.
10. Bathnagar A, Sillanpää M. Utilization of agro-industrial and municipal waste materials as potential adsorbents for water treatment— A review. Chem. Eng. J. 2010;157:277-296.
11. Sud D, Mahajan G, Kaur MP. Agricultural waste material as potential adsorbent for sequestering heavy metal ions from aqueous solutions— A review. Bioresource Technology. 2008;99:6017-6027.
12. Kurniawan TA, Chan GYS, Lo WH, Babel S. Comparison of low-cost adsorbents for treating wastewater laden with heavy metals, Sci. total Environ. 2006;366:409-426.
13. Hua M, Zhang S, Pan B, Zhang W, Lv L, Zhang Q. Heavy metal removal from water/wastewater by nanosized metal oxides: A review, J. Hazard. Mater. 2012;211-212:317-331 and references therein.
14. Han R, Zou W, Li H, Li Y, Shi J, Copper(II) and lead(II) removal from aqueous solution in fixed-bed columns by manganese oxide coated zeolite, J. Hazard. Mater. 2006;B137: 934-942.
15. Zou W, Han R, Chen Z, Jinghua Z, Shi J. Kinetic study of adsorption of Cu(II) and Pb(II) from aqueous solutions using manganese oxide coated zeolite in batch mode, Colloids and Surfaces A: Physicochem. Eng. Aspects. 2006;279:238-246.
16. Han R, Zou L, Zhao X, Xu Y, Xu F, Li Y, Wang Y. Characterization and properties of iron oxide-coated zeolite as adsorbent for removal of copper(II) from solution in fixed bed column, Chem. Eng. J. 2009;149:123-131.
17. Dehou SC, Wartel M, Recourt P, Revel B, Mabingui J, Montiel A, Boughriet A. Physicochemical, crystalline and morphological characteristics of bricks used for ground waters purification in Bangui region (Central African Republic). Applied Clay Science. 2012a;59-60:69-75.
18. Dehou SC, Wartel M, Recourt P, Revel B, Boughriet A. Acid treatment of crushed brick (from Central African Republic) and its ability (after FeOOH coating) to adsorb ferrous ions from aqueous solutions. The open Materials Science Journal. 2012b;6:50-59.

19. Dehou SC, Mabingui J, Lesven L, Wartel M, Boughriet A. Improvement of Fe(II)-adsorption capacity of FeOOH-coated brick in solutions, and kinetics aspects, Journal of Water Resource and Protection. 2012c;4:464-473.
20. Allahdin O, Dehou SC, Wartel M, Recourt P, Trentesaux M, Mabingui J, Boughriet A. Performance of FeOOH-brick based composite for Fe(II) removal from water in fixed bed column and mechanistic aspects, Chem. Eng. Res. Design. 2013;91:2732-3742.
21. Allahdin O, Wartel M, Recourt P, Revel B, Ouddane B, Billon G, Mabingui J, Boughriet A. Adsorption capacity of iron oxihydroxide-coated brick for cationic metals and nature of ion surface interactions, Applied Clay Science. 2014, in press Available: http://dx.doi.org/10.1016/j.clay.2014.01.008.
22. Stumm W, Morgan JJ. Aquatic Chemistry: Chemical Equilibria and Rates in Natural Waters. Third Edition. Environmental Science and Technology. John Wiley & Sons, INC., New York. 1996;461.
23. Freundlich HMF. Over the adsorption in solution, J. Phys. Chem. 1906;57:385-471.
24. Langmuir I. The construction and fundamental properties of solids and liquids. J. Am. Chem. Soc. 1916;38(11):2221-2295.
25. Hill AV. The possible effects of the aggregation of the molecules of haemoglobin on its dissociation curves. J. Physiol. (London). 1910;40:4-7.
26. Tempkin MI, Pyzhev V. Kinetics of ammonia synthesis in promoted iron catalyst. Acta Phys. Chim. USSR. 1940;12:327-356.
27. Sips R. Combined form of Langmuir and Freundlich equations, J. Chem. Phys. 1948;16:490-495.
28. Dubinin MM, Radushkevich LV. The equation of the characteristic curve of the activated charcoal, Proc. Acad. Sci. USSR Phys. Chem. 1947;55:331-337.
29. Redlich O, Peterson DL. A useful adsorption isotherm. J. Phys. Chem. 1959;63:1024-1026.
30. Toth J. State equations of the solid gas interface layer, Acta Chem. Acad. Hung. 1971;69:311-317.
31. Horsfall M, Spiff AI. Equilibrium sorption study of Al^{3+}, Co^{2+} and Ag^{2+} in aqueous solutions by fluted pumpkin (*Telfairia occidentalis* HOOK) waste biomass. Acta Chim. Slov. 2005;52:174-181.
32. Vijayaraghavan K, Padmesh TVN, Palanivelu K, Velan M, Bisorption of nickel(II) ions onto *Sargassum wightii:* application of two-parameter and three parameter isotherm models. J. Hazard. Mater. 2006; B133: 304-308.
33. Foo KY, Hameed BH. Insights into the modeling of adsorption isotherm systems, Chem. Eng. J. 2010;156:2-10. and references therein.
34. Bulut E, Ozacar M, Sengil IA. Adsorption of malachite green onto bentonite: equilibrium and kinetic studies and process design, Micropor. Mesopor. Mater. 2008;115:234-246.
35. Huang YH, Hsueh CL, Huang CP, Su LC, Chen CY. Adsorption thermodynamic and kinetic studies of Pb(II) removal from water onto a versatile Al_2O_3-supported iron oxide, Sep. Purif. Technol. 2007;55:23-29.
36. Eren E. Removal of lead ions by Unye (Turkey) bentonite in iron and magnesium oxide-coated forms, J. Hazard. Mater. 2009;165:63-70.
37. Lai CH, Chen CY. Removal of metal ions and humic acid from water by iron-coated filter media, Chemosphere. 2001;44:1177-1184.
38. Boujelben N, Bouzid J, Elouear Z. Adsorption of nickel and copper onto natural iron-oxide-coated sand from aqueous solutions: study in single and binary systems. J. Hazard. Mater. 2009;163:376-382.
39. Phuengprasop T, Sittiwong J, Unob F. Removal of heavy metal ions by iron oxide coated sewage sludge, J. Hazard. Mater. 2011;186:502-507.

40. Unob F, Wongsiri B, Phaeon N, Puanngam M, Shiowatana J. Reuse of waste silica as adsorbent for metal removal by iron oxide modification. J. Hazard. Mater. 2007;142:455-462.
41. Eren E, Gumus H. Characterization of the structural properties and Pb(II) adsorption behavior of iron oxide coated sepiolite, Desalination. 2011;273:276-284.
42. Lai CH, Chen CY, Wei BL, Lee CW. Adsorptive characteristics of cadmium and lead on the goethite-coated sand surface, J. Environ. Sci. Health. 2001;A36:741-763.
43. Lai CH, Chen CY, Wei BL, Yeh SH. Cadmium adsorption on goethite-coated sand in the presence of humic acid, Water Res. 2002;36:4943-4950.
44. Lai CH, Chen CY. Removal of metal ions and humic acid from water by iron-coated flter media, Chemosphere. 2001;44:1177-1184.
45. Doula MK. Simultaneous removal of Cu, Mn and Zn from drinking water with the use of clinoptilolite and its Fe-modified form. Water Res. 2009;4:3659-3672.
46. Manju GN, Krishnan KA, Vinod VP, Anirudhan TS. An investigation into the sorption of heavy metals from wastewaters by polyacrylamide-grafted iron(III) oxide, J. Hazard. Mater. 2002;91:221-238.
47. Randelović M, Purenović M, Zarubica A, Purenović J, Matović B, Momčilovič M. Synthesis of composite by application of mixed Fe, Mg (hydr)oxides coatings onto bentonite—A use for the removal of Pb(II) from water, J. Hazard., Mater. 2012;199-200:367-374.
48. Gupta SS, Bhattacharyya KG. Kinetics of adsorption of metal ions on inorganic materials: A review, Advances in Colloid and Interface Science. 2011;162:39-59.
49. Lagergren S. Zurtheorie der sogenannten adsorption gelosterstoffe. Kung-liga Svenska Vetenkapsakademiens, Handlingar. 1898;24(4):1-39.
50. Ho YS, Mckay G. Comparative sorption kinetic studies of dye and aromatic compounds onto fly ash, J. Environ. Sci. Health. 1999;A34(5):1179-1204.
51. Unuabonah RI, Adebowale KO, Owolabi BI. Kinetic and thermodynamic studies of the adsorption of lead (II) ions onto phosphate-modified kaolinite clay. J. Hazard. Mater. 2007;144:386-395.
52. Ozcan A, Ozcan AS, Gok O. Adsorption kinetics and isotherms of anionic dye of reactive blue 19 from aqueous solutions onto DTMA-sepiolite, in: A. A. Lewinsky (Ed.), Hazardous Materials and Wastewater—Treatment, Removal and Analysis. Nova Science Publishers, New York; 2007.
53. Boparai HK, Joseph M, O'Carroll DM. Kinetics and thermodynamics of cadmium ion removal by adsorption onto nanozerovalent iron particles. J. Hazard. Mater. 2011;186:458-465.
54. Özcan A, Öncü EM, Özcan AS. Adsorption of Acid Blue 193 from aqueous solutions onto DEDMA-Sepiolite, J. Hazard. Mater. 2006;B129:244-252.
55. Li Y, Yue Q, Gao B, Li Q, Li C. Adsorption thermodynamic and kinetics studies of dissolved chromium onto humic acids, Colloids and Surfaces B. Biointerfaces. 2008;65:25-29, and references therein.
56. Largitte L, Lodewyckx P. Studying different methods to determine the thermo kinetic constants in the adsorption of Pb^{2+} on an activated carbon from Bois carré seeds, J. Environ. Chem. Eng. 2014; in press.
Available: http://dx.doi.org/10.1016/j.jece.2014.02.001 and references therin.
57. Petrou AL. The free energy of activation as the critical factor in geochemical processes, Chem. Geology. 2012;308-309:50-59.
58. Mohapatra M, Khatun S, Anand S. Kinetics and Thermodynamics of lead(II) adsorption on lateritic nickel ores of Indian origin, Chem. Eng. J. 2009;155:184-190.
59. Scheckel KG, Sparks DC. Temperature effect on nickel sorption kinetics of the mineral-water interface, Soil Sci. Soc. Am. J. 2001;65:719-728.

60. Dogan M, Alkan M. Adsorption kinetics of methyl violet onto perlite, Chemosphere. 2003;50:517-528.
61. Gu X, Les J. Evans, Surface complexation modelling of Cd(II), Cu(II), Ni(II), Pb(II) and Zn(II) adsorption onto kaolinite, Geochim. Cosmochim. Acta. 2008;72:267-276.
62. Charlot G. L'Analyse Qualitative et les Réactions en Solution, Masson & Cie, Paris. 1963;442.
63. Martell AE, Smith RM. NIST standard reference database 46 version 7.0. NIST, Gaithersburg, US; 2004.
64. Wiese GR, James RO, HEALY TW. Discreteness of charge and solvation effects in cation adsorption at the oxide/water interface, Discuss. Faraday Soc. 1971;52:302-311.

Peer-review history:
The peer review history for this paper can be accessed here:
http://www.sciencedomain.org/review-history.php?iid=475&id=16&aid=4574